# Continuous Olefin Copolymerization with Soluble Ziegler-Natta Catalysts

**Kee Jeong Kim and Kyu Yong Choi**
Dept. of Chemical Engineering and Systems Research Center, University of Maryland, College Park, MD 20742

Soluble transition metal catalysts, such as $VOCl_3$/aluminum alkyls, have been used in the polyolefin industry for many years to produce ethylene homopolymers and copolymers. Here, the catalyst is soluble in the liquid phase where monomers and solvents or diluents are present. Depending on the reactor temperature and copolymer composition, polymers produced may precipitate as solids or may remain dissolved in the fluid phase. The polymerization activity of modern soluble catalysts is so high that the removal of catalyst residues is not required after polymerization, and relatively small reactors with short residence time can be used.

Although there is a plethora of literature available concerning the polymerization kinetics and mechanisms for various heterogeneous and homogeneous Ziegler-Natta catalysts, very little has been reported on the modeling of continuous polymerization reactors with soluble or homogeneous catalysts (Choi, 1985; Cozewith, 1988). Recently, Cozewith (1988) investigated the transient response of continuous stirred tank reactors for the polymerization of ethylene/propylene/diene copolymers (EPDM) with soluble $VOCl_3/Et_3Al_2Cl_3$ catalyst. Using a detailed kinetic model, he showed that the dynamic response of polymer molecular weight and copolymer composition is relatively slow and that response time depends on the direction and magnitude of changes in some reactor operating conditions. The model simulations with a single-site catalytic reaction mechanism have been shown to agree very well with experimental data.

In this note, we examine the steady-state and dynamic behavior of a continuous stirred tank reactor (CSTR) for the copolymerization of ethylene and butene-1 with soluble catalysts. The soluble Ziegler-Natta catalyst considered in this study is a proprietary high-activity industrial catalyst used in conjunction with aluminum alkyl cocatalyst. This catalyst exhibits rapid decay during the polymerization, and its deactivation rate increases as the reaction temperature increases. The catalyst is also known to have only one active catalytic species. It is used for the synthesis of olefin homopolymers and copolymers in a broad range of polymerization temperature so that a variety of polymer grades can be readily obtained.

Correspondence concerning this note should be addressed to K. Y. Choi.

## Reactor Model

The polymerization reactor to be modeled is an ideal, backmixed, continuous stirred tank reactor with a cooling jacket. A feed stream consists of ethylene $M_1$ and higher $\alpha$-olefin comonomer $M_2$ such as butene-1, which is much less reactive than ethylene. A small amount of preactivated catalyst solution is supplied from a separate storage tank and mixed with the monomers near the inlet of the reactor before being injected to the reactor. The feed stream temperature is sufficiently low to prevent a premature polymerization near the reactor inlet. The copolymerization kinetics are characterized by very rapid chain initiation and catalyst deactivation leading to a substantial loss of catalyst activity. However, the overall catalyst activity (kg polymer/g catalyst) is so high that a good yield of copolymers is obtainable in relatively short residence time. In the absence of added chain transfer agents, the polymer chains stop to grow via catalyst deactivation and chain transfers to monomers and aluminum alkyl cocatalyst, and spontaneous chain transfer reactions. It is assumed that no impurities are present in the feed. Table 1 shows a kinetic scheme for the copolymerization of $\alpha$-olefins used in our reactor modeling. The symbols used in Table 1 are defined in Notation.

Assuming ideal backmixing in the reactor, one can derive a following dynamic reactor model:

$$\frac{dM_1}{dt}=\frac{1}{\tilde{\tau}}(M_{1f}-M_1)-(k_{11}P+k_{21}Q)M_1 \tag{1}$$

$$\frac{dM_2}{dt}=\frac{1}{\tilde{\tau}}(M_{2f}-M_2)-(k_{12}P+k_{22}Q)M_2 \tag{2}$$

$$\frac{dP_T}{dt}=\frac{1}{\tilde{\tau}}(C_f^*-P_T)-k_dP_T \tag{3}$$

$$\frac{dT}{dt}=\frac{1}{\tilde{\tau}}(T_f-T)+\frac{(-\Delta H_1)}{\rho C_p}(k_{11}P+k_{21}Q)M_1 + \frac{(-\Delta H_2)}{\rho C_p}(k_{12}P+k_{22}Q)M_2-\frac{U_c}{\rho C_pV}(T-T_c) \tag{4}$$

where $\tilde{\tau}$ is the residence time and the subscript $f$ denotes the

**Table 1. Kinetic Scheme for $\alpha$-Olefin Copolymerization**

| | |
|---|---|
| *Chain Initiation* | |
| $C^* + M_1 \xrightarrow{k_{i1}} P_{1,0}$ | (A1) |
| $C^* + M_2 \xrightarrow{k_{i2}} Q_{0,1}$ | (A2) |
| *Chain Propagation* | |
| $P_{n,m} + M_1 \xrightarrow{k_{11}} P_{n+1,m}$ | (B1) |
| $P_{n,m} + M_2 \xrightarrow{k_{12}} Q_{n,m+1}$ | (B2) |
| $Q_{n,m} + M_1 \xrightarrow{k_{21}} P_{n+1,m}$ | (B3) |
| $Q_{n,m} + M_2 \xrightarrow{k_{22}} Q_{n,m+1}$ | (B4) |
| *Chain Transfer* | |
| $P_{n,m} + M_1 \xrightarrow{k_{f11}} M_{n,m} + P_{1,0}$ | (C1) |
| $P_{n,m} + M_2 \xrightarrow{k_{f12}} M_{n,m} + Q_{0,1}$ | (C2) |
| $Q_{n,m} + M_1 \xrightarrow{k_{f21}} M_{n,m} + P_{1,0}$ | (C3) |
| $Q_{n,m} + M_2 \xrightarrow{k_{f22}} M_{n,m} + Q_{0,1}$ | (C4) |
| $P_{n,m} + Al \xrightarrow{k_{f1Al}} M_{n,m} + C^*$ | (C5) |
| $Q_{n,m} + Al \xrightarrow{k_{f2Al}} M_{n,m} + C^*$ | (C6) |
| $P_{n,m} \xrightarrow{k_{f1}} M_{n,m} + C^*$ | (C7) |
| $Q_{n,m} \xrightarrow{k_{f2}} M_{n,m} + C^*$ | (C8) |
| *Catalyst Deactivation* | |
| $C^* \xrightarrow{k_{dc}} D^*$ | (D1) |
| $P_{n,m} \xrightarrow{k_{d1}} M_{n,m} + D^*$ | (D2) |
| $Q_{n,m} \xrightarrow{k_{d2}} M_{n,m} + D^*$ | (D3) |

**Table 2. Numerical Values of Kinetic and Physical Parameters**

| | |
|---|---|
| *Kinetic Parameters* | |
| $k_{11} = 5.8 \times 10^{13}\exp(-4{,}900/RT)$L/mol·h | |
| $k_{12} = 2.6 \times 10^{12}\exp(-4{,}900/RT)$L/mol·h | |
| $k_{21} = 1.7 \times 10^{14}\exp(-6{,}200/RT)$L/mol·h | |
| $k_{22} = 3.8 \times 10^{12}\exp(-6{,}200/RT)$L/mol·h | |
| $k_d = 1.7 \times 10^{8}\exp(-6{,}000/RT)h^{-1}$ | |
| $k_{f11} = 2.1 \times 10^{8}\exp(-3{,}475/RT)$L/mol·h | |
| $k_{f12} = 1.7 \times 10^{-2} k_{f11}$L/mol·h | |
| $k_{f21} = 9.8 \times 10^{7}\exp(-4{,}777/RT)$L/mol·h | |
| $k_{f22} = 3.0 \times 10^{-2} k_{f22}$L/mol·h | |
| $k_{f1Al} = 2.1 \times 10^{9}\exp(-3{,}475/RT)(\text{mol/L})^{1/2}/h$ | |
| $k_{f2Al} = 1.7 \times 10^{-2} k_{f1Al}(\text{mol/L})^{1/2}/h$ | |
| $k_{f1} = 1.8 \times 10^{14}\exp(-11{,}095/RT)h^{-1}$ | |
| $k_{f2} = 4.9 \times 10^{15}\exp(-12{,}395/RT)h^{-1}$ | |
| *Physical and Reactor Design Parameters* | |
| $\Delta H_1 = -22.66$ kcal/mol | $\Delta H_2 = -20.26$ kcal/mol |
| $\rho C_p = 0.3$ kcal/l°C | $U_c = 31.5$ kcal/h·K |
| $\Theta_f = 0.17$ | $\Theta_c = 0.6$. |
| *Physical and Reactor Design Parameters* | |
| $T_r = 300$ K | $R_{p,r} = 9{,}000$ mol/L·h |
| $A_{c,r} = 180$ kg polymer/g cat | $C^*_{f,r} = 6.6 \times 10^{-7}$mol/L |
| $M_{n,r} = 10{,}000$ | |

feed condition. $P$ and $Q$ are the total concentrations of the copolymer species, $P_{n,m}$ and $Q_{n,m}$. $P_{n,m}$ is the growing polymer chains having $n$ units of $M_1$ and $m$ units of $M_2$ with $M_1$ attached to active transition metal site. $Q_{n,m}$ is defined similarly. $P_T$ is the total concentration of active catalytic sites (transition metal species) in the reactor ($P_T = P + Q + C^*$). It is assumed that the physical constants, heat of reactions ($\Delta H_1$ and $\Delta H_2$), and the effective heat transfer coefficient $U_c$ are constant in the temperature range of interest. Note in Table 1 that reactions B1 and B3 and reactions B2 and B4 are assumed to have the same heat of reaction so that only two reaction heats are needed in the above energy balance equation. Pressure variations in the reactor during the reaction are assumed negligible. Also note that the first-order catalyst deactivation kinetics is used and it is assumed that $k_{dc} \approx k_{d1} \approx k_{d2} = k_d$. For the calculation of copolymer molecular weight, the first three leading moments for dead polymers are used. The derivation of the moment equations is straightforward following the techniques described by Ray (1972).

In calculating the molecular weight moments, we applied a quasi steady-state approximation (QSSA) to live polymers. Our separate simulations of the kinetic model without using the QSSA indicated that there was no discernible difference in the simulation results from those with the QSSA. A computational load is reduced considerably when the QSSA is used for the model simulations. Since the concentrations of live polymers are far smaller than those of dead polymers, the polymer molecular weight averages are calculated using the dead polymer moments only. In the above model, no chain transfer agents such as hydrogen are assumed to be present in the feed stream. If necessary, however, a hydrogen chain transfer mechanism can be added to the kinetic model easily. The numerical values of kinetic parameters and physical constants used in our model simulations are listed in Table 2. These kinetical parameters were obtained from the industrial pilot-plant data with the catalyst system considered in this work.

In manufacturing high- or low-density polyolefins, it is of particular importance to control the key copolymer properties such as polymer molecular weight, polydispersity, and copolymer density. The control of copolymer density is achieved by controlling the copolymer composition. The main objective of the reactor analysis to follow is to illustrate the effect of reactor operating conditions on the reactor performance both in the steady state and the transient state. Some of the process variables shown in the following figures are normalized by their corresponding reference values, as defined in Notation.

## *Steady-state behavior*

The steady-state profiles of various reactor state variables and copolymer properties for varying residence time are shown in Figure 1 for a standard set of reactor operating conditions listed in Table 2. Here, the residence time $\tau$ is expressed as a multiple of a standard reactor residence time $\bar{\tau}_r$. The feed monomer mole ratio ($\phi_f = M_{2f}/M_{1f}$) is fixed at 1.0. Figure 1a shows that the steady-state reactor temperature $\Theta$ increases with an increase in residence time and reaches a maximum value at $\tau = 2.6$ and then decreases gradually as the residence time is further increased. Figure 1a also shows the concentration profile of active propagating centers $\Psi$ in the reactor. With an increase in residence time and reactor temperature, $\Psi$ decreases significantly due to the loss of active sites by catalyst deactivation reaction.

When the reactor residence time is very short ($\tau < 0.6$), the polymerization rates for each monomer ($R_1$ and $R_2$) increase with increasing residence time, because in this operating region the intrinsic site activity increases markedly with temperature, and the loss of active propagating centers is not significant. However, as $\tau$ exceeds 0.6, the reactor temperature continues

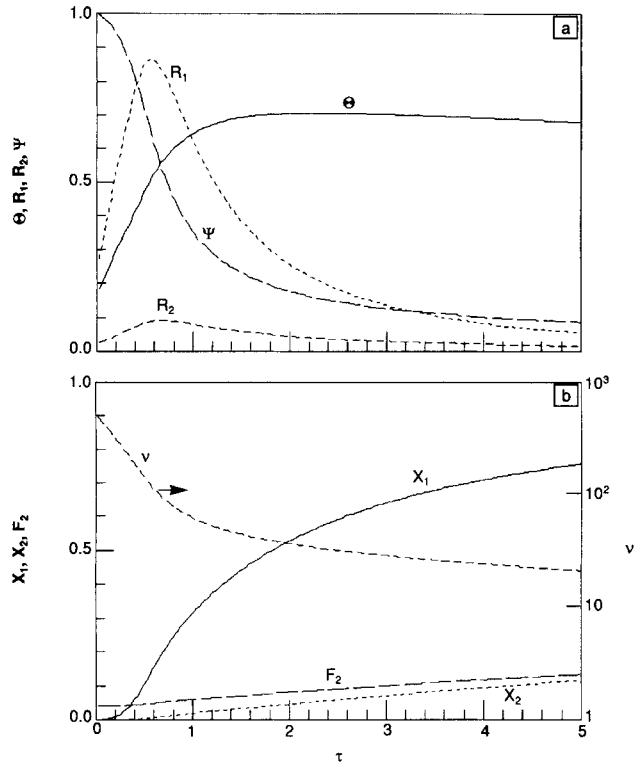


**Figure 1. Steady-state profiles of reactor variables and copolymer property parameters for $\phi_f = 1.0$ with deactivating catalyst.**

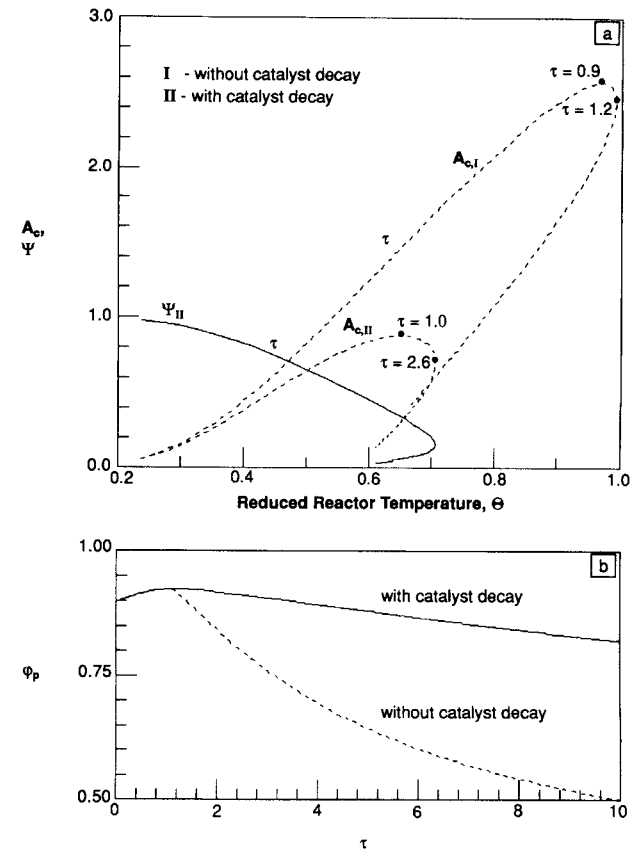


**Figure 2. (a) Effect of steady-state temperature on catalyst activity $A_c$, active propagating site concentration $\Psi$; (b) fraction of $P$-sites for deactivating and nondeactivating catalysts, $\phi_f = 1.0$.**

to increase and the loss of active sites has a more significant impact on the overall reaction rate than the increase in the site activity. As a result, the polymerization rates for $M_1$ and $M_2$ ($R_1$ and $R_2$) decrease as residence time is further increased, although the reactor temperature is high.

The similar behavior of decreasing catalyst activity with an increase in reactor temperature, due to catalyst deactivation, has been reported for some high-activity soluble transition metal catalysts used in homogeneous solution polymerization processes (Agapiou and Etherton, 1988; Machon, 1988; Chien and Bres, 1986). Figure 1b shows the conversions of $M_1$ ($X_1$) and $M_2$ ($X_2$), mole fraction of $M_2$ in the copolymer ($F_2$), and the reduced copolymer molecular weight ($\nu$). Note that the decrease in the polymer molecular weight with an increase in the reactor residence time is quite substantial.

It is well known that for many exothermic polymerization processes including heterogeneously-catalyzed olefin polymerization processes, steady-state multiplicity and runaway reactions may occur under certain operating conditions (Choi and Ray, 1985c, 1988). However, in the range of reactor operating conditions considered in this work, only stable and unique steady states exist. This is because as the reactor temperature increases, the catalyst deactivation rate also increases, while the polymerization rate and the amount of heat release decrease. As a result, no steady-state bifurcation occurs to multiple steady state, and runaway reaction is highly unlikely to occur with this deactivating catalyst.

The effect of the steady-state reactor temperature on the catalyst activity and the concentration of active propagating centers is shown in Figure 2a for deactivating and nondeactivating catalysts. Here, the activity parameter $A_c$ is the catalyst activity normalized by a standard catalyst activity of 180 kg polymer/g catalyst, which is a typical value for modern high-activity catalysts. The arrows in the curves indicate the direction of increasing reactor residence time $\tau$. The activity of nondeactivating catalyst $A_{c,I}$ increases with increasing reactor temperature up to $\tau = 0.9$, where the catalyst exhibits a maximum activity. As the residence time is further increased from the peak point, the catalyst activity begins to fall even though the reactor temperature continues to increase. At $\tau = 1.2$, the reactor temperature also starts to decrease. This is because the conversions of $M_1$ and $M_2$ are high, and only small amounts of unreacted monomers are left in the reactor, resulting in the reduced polymerization rate. When there is a significant catalyst deactivation, the catalyst activity $A_{c,II}$ increases with an increase in the reaction temperature for $\tau$ up to 1.0; however, the overall catalyst activity is lower than that of nondeactivating catalyst. Note that the concentration of active propagating centers ($\Psi_{II}$) decreases sharply as the reactor temperature is increased. For the deactivating catalyst, the reactor temperature continues to increase for $\tau$ up to $\tau = 2.6$, although the overall catalyst activity decreases for $\tau > 1.0$.

Figure 2b shows for both nondeactivating and deactivating catalysts the fraction of $P$-sites [$\varphi_p = P/(P + Q)$] where $M_1$ monomers are attached to active transition metals. For the

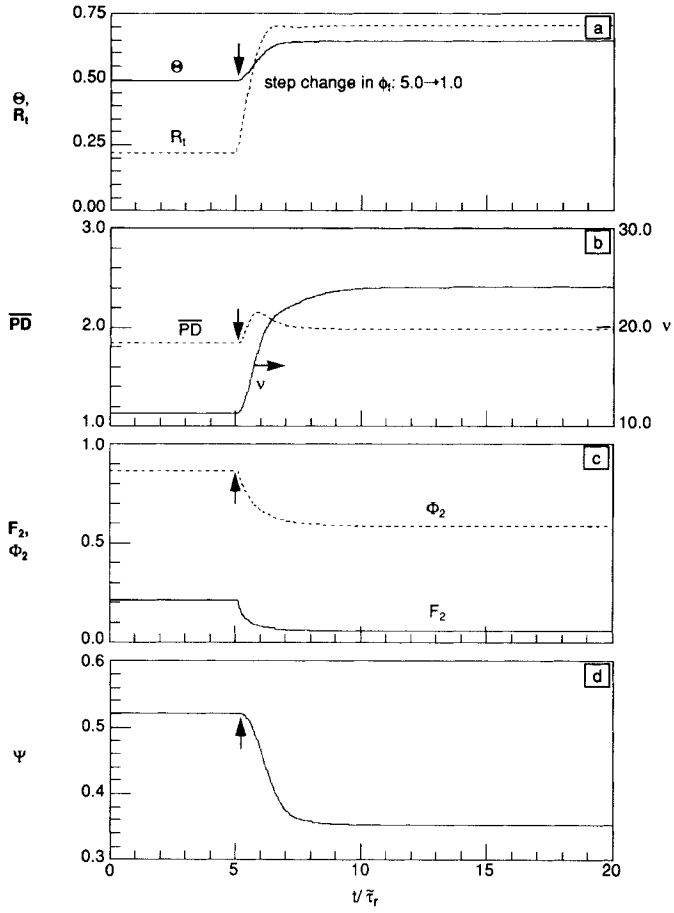


**Figure 3. Open-loop reactor transients to a step change in feed monomer mole ratio from 5.0 to 1.0 ($\tau = 1.0$).**

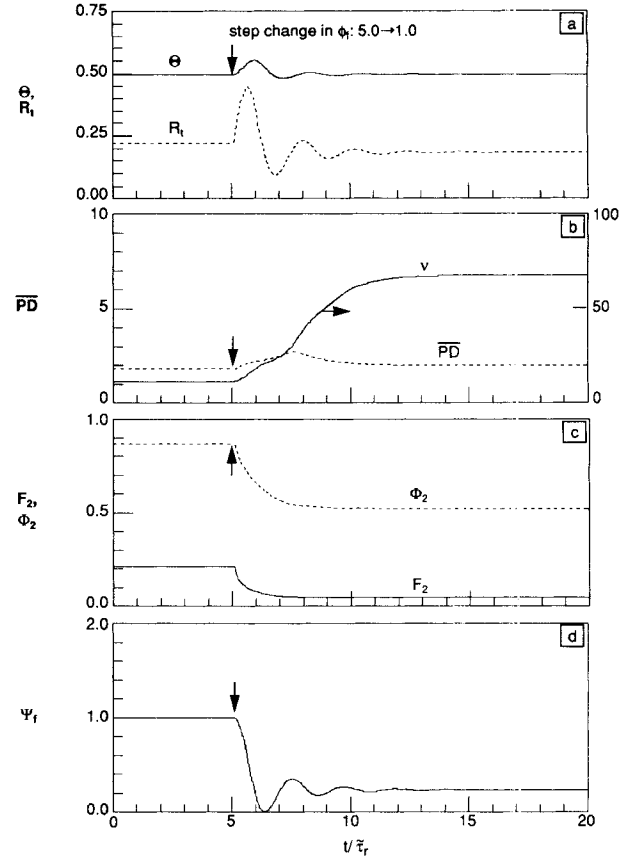


**Figure 4. Closed-loop reactor transients to a step change in feed monomer mole ratio from 5.0 to 1.0($\tau = 1.0$).**

$K_c = 0.02$L/h·°C, $\tau_I = 150$ h

range of reactor residence time considered ($0 < \tau < 10$), there are more $P$-sites than $Q$-sites. $\varphi_p$ increases slightly as the residence time is increased up to about $\tau = 1.0$, but as $\tau$ exceeds 1.0 the fraction of $P$-sites begins to fall. This is because as $\tau$ increases, the reactor temperature increases and $M_1$ is consumed much faster than $M_2$. Since the ratio of the cross-propagation rate constants ($k_{12}/k_{21}$) is not as sensitive to the reactor temperature as the monomer mole ratio, the fraction of $P$-site given by

$$\varphi_p = \frac{1}{1 + \frac{k_{12}}{k_{21}} \frac{M_2}{M_1}} \tag{5}$$

decreases as the polymerization rate increases. Figure 2b indicates that for $\tau > 1.0$ the fraction of $P$-sites for deactivating catalyst is higher than that for nondeactivating catalyst. For a given $\tau$, the steady-state temperature is higher for nondeactivating catalyst than for deactivating catalyst. Therefore, the monomer mole ratio in the reactor ($\phi = M_2/M_1$) is much higher for nondeactivating catalyst than for the deactivating catalyst.

### *Open-loop transient behavior*

An understanding of open-loop reactor dynamics is important in designing a reactor control system to produce the polymers of desired properties. In the following, we shall show the reactor response for the transition from one steady-state operating point to another following a step change in feed conditions.

The reactor response to a step decrease in the feed monomer ratio $\phi_f$ from 5.0 to 1.0 is shown in Figure 3. Here, the total monomer feed rate is held constant, and only the feed monomer ratio is changed. In practice, the desired copolymer density is obtained by regulating the monomer mole ratio in the reactor. Since more reactive ethylene $M_1$ is present in much larger proportion when $\phi_f$ is decreased from 5.0 to 1.0, the reactor temperature and overall polymerization rate increase significantly. In general, polymer molecular weight decreases as the reactor temperature is increased. When the monomer mole ratio is decreased, however, the copolymer molecular weight increases by 70% because more $M_1$ monomers, which are more reactive than $M_2$, are incorporated into the copolymer.

Figure 3 also shows that about five reactor turnovers are needed to reach new steady-state molecular weight and three reactor turnovers for copolymer composition. The polydispersity reaches a new steady state in about three reactor turnovers. Cozewith (1988) reported that for the EPDM polymerization reactor system response time depends on the direction and the magnitude of change and is generally shorter when a property value such as polymer molecular weight is

decreased. In our cases, both the catalyst site concentration and the comonomer mole fraction in the polymer $F_2$ reach the new steady state faster with a reduction in these values than with an increase. It is also interesting to note from Figure 3 that the polydispersity ($\overline{PD} = M_w/M_n$) increases slightly during the transient period.

### *Closed-loop transient behavior*

The temperature of the copolymerization reactor is controlled by adjusting the catalyst injection rate or the catalyst concentration in the feed stream. The copolymer composition can be controlled by manipulating the feed comonomer composition. It, however, is very difficult to measure on-line due to the lack of efficient on-line sensors. Thus, the copolymer composition is controlled indirectly by feeding the comonomer of the prespecified composition that will give a desired final copolymer composition. In the following, we will illustrate the reactor transients with temperature control only.

Figure 4 shows the closed-loop transient response of the reactor operating at standard residence time ($\tau = 1.0$) to a step change in $\phi_f$ from 5.0 to 1.0 with a proportional-integral (PI) temperature controller. The controller parameters (gain and reset rate) were determined using the Ziegler-Nichols tuning rules with a linearized process model and its open-loop step testing data. Some adjustments of the tuning parameters have been made to obtain a good closed-loop control performance. Figure 4a shows the temperature and reaction rate responses, and Figure 4d shows the profiles of normalized catalyst feed concentration $\Psi_f$ used as a manipulated variable. (In actual process, the catalyst injection rate is manipulated.) As the feed monomer ratio ($\phi_f = M_{2f}/M_{1f}$) is decreased, more reactive $M_1$ monomer is present in the feed in a large proportion, and therefore the catalyst injection rate is reduced to control the reactor temperature. Figures 4a and 4d show that the catalyst injection rate is an effective manipulated variable to control the temperature. Figure 4a also indicates that the overall copolymerization rate increases immediately after the change in the feed mole ratio, but reaches the new steady-state value, which is slightly lower than the original value, in about five reactor turnovers.

Polymer molecular weight $\nu$ increases to a new steady-state value in about nine reactor turnovers, whereas the copolymer composition $F_2$ and the mole fraction of $M_2$ in the bulk phase $\Phi_2$ decrease to new steady-state values in less than three reactor turnovers. Compared with the open-loop response for the same change in $\phi_f$ (Figure 3), the closed-loop molecular weight $\nu$ response shows some noticeable differences.

1. The closed-loop polymer molecular weight response is much slower than the open-loop response.

2. The steady-state polymer molecular weight is much higher than that in the open-loop case.

When the reactor temperature is forced to remain at the original temperature by reducing the feed catalyst concentration, the total polymerization rate is also suppressed and thus the chain growth reaction is retarded. Apparently, the effect of increased chain transfer reactions to ethylene $M_1$ (for example, Eqs. C1 and C3 in Table 1) by the step change in $\phi_f$ from 0.5 to 1.0 is much smaller than that of chain growth reaction at the controlled temperature, which is much lower than the open-loop steady-state temperature. As a result, much higher molecular weight polymers are obtained in the closed-loop system. The polydispersity $\overline{PD}$ reaches a new steady state in five reactor turnovers. Note that during the transient period, polydispersity increases, but the final $\overline{PD}$ value is still very close to 2.0. The simulation results shown in Figure 4 clearly indicate that the polymer properties vary significantly even though the temperature is perfectly controlled. This is because the reactor is operating at a new steady state.

## Acknowledgment

Financial support provided by the National Science Foundation (CBT-85-52428) and EXXON Chemical Company are gratefully acknowledged.

## Notation

$A_c$ = reduced catalyst activity parameter, $A_{c,0}/A_{c,r}$
$C^*$ = concentration of empty active catalyst sites, mol/L
$D^*$ = concentration of permanently deactivated sites, mol/L
$F_2$ = mole fraction of $M_2$ in copolymer
$k_d$ = rate constants of spontaneous catalyst deactivation, $h^{-1}$
$k_{fi}$ = rate constants of spontaneous chain transfer, for $i = 1, 2$, $hr^{-1}$
$k_{fiAl}$ = rate constants of chain transfer to cocatalyst, for $i = 1, 2$, $(mol/L)^{1/2}/h$
$k_{fij}$ = rate constants of chain transfer to monomer, for $i, j = 1, 2$, L/mol·h
$k_{ij}$ = propagation rate constants, for $i, j = 1, 2$, L/mol·h
$M_1$ = concentration of ethylene monomer, mol/L
$M_2$ = concentration of high $\alpha$-olefin comonomer, mol/L
$M_n$ = number average molecular weight
$M_w$ = weight average molecular weight
$P$ = total concentration of $P_{n,m}$, mol/L
$P_{n,m}$ = concentration of growing copolymer chains bounded by $M_1$ having $n$ unit of $M_1$ and $m$ units of $M_2$, mol/L
$P_T$ = total concentration of active propagating centers, mol/L
$\overline{PD}$ = polydispersity of the polymer, $M_w/M_n$
$Q$ = total concentration of $Q_{n,m}$, mol/L
$Q_{n,m}$ = concentration of growing copolymer chains bounded by $M_2$ having $n$ units of $M_1$ and $m$ units of $M_2$
$R_1$ = reduced copolymerization rate of $M_1$, $R_{p1}/R_{p,r}$
$R_2$ = reduced copolymerization rate of $M_2$, $R_{p1}/R_{p,r}$
$R_p$ = total copolymerization rate, mol/L·h
$R_{p1}$ = copolymerization rate of $M_1$, mol/L·h
$R_{p2}$ = copolymerization rate of $M_2$, mol/L·h
$R_t$ = reduced total copolymerization rate, $R_{p1}/R_{p,r}$
$T$ = reactor temperature, K
$T_c$ = coolant temperature, K
$T_f$ = feed temperature, K
$t$ = time, min
$U_c$ = effective heat transfer coefficient, kcal/h·K
$V$ = reactor volume, L
$X_1$ = fractional conversion of $M_1$
$X_2$ = fractional conversion of $M_2$

### *Greek letters*

$\Theta$ = reduced reactor temperature, $T/T_r$
$\Theta_c$ = reduced coolant temperature, $T_c/T_r$
$\Theta_f$ = reduced feed temperature, $T_f/T_r$
$\nu$ = reduced number average molecular weight, $M_n/M_{n,r}$
$\rho C_p$ = heat capacity of reaction mixture, kcal/L·K
$\tau$ = reduced reactor residence time, $\tilde{\tau}/\tilde{\tau}_r$
$\tilde{\tau}$ = reactor residence time, h
$\tilde{\tau}_r$ = standard reactor residence time, h
$\Phi_2$ = mole fraction of $M_2$ in bulk phase
$\phi_f$ = feed monomer mole ratio, $(M_2/M_1)_f$
$\varphi_p$ = fraction of $P$-sites, $P/(P+Q)$
$\Psi$ = reduced concentration of active propagating centers, $P_T/C_f^*$

### *Subscript*

$f$ = feed condition
$r$ = reference condition

## Literature Cited


Agapiou, A. K., and B. P. Etherton, "Development of High-Pressure/High-Temperature Transition Metal Catalysts for Ethylene (Co)Polymerizations," *Transition Metal Catalyzed Polymerizations*, p. 364 R. P. Quirk, ed., Cambridge Univ. Press, Cambridge, U.K. (1988).

Chien, J. W. C., and P. L. Bres, "Magnesium-Chloride-Supported High-Mileage Catalysts for Olefin Polymerization: XII. Polymerization of Ethylene," *J. Polym. Sci.: Part A. Polym. Chem.*, **24**, 2483 (1986).

Choi, K. Y., "Control of Molecular Weight Distribution of Polyethylene in Continuous Stirred Tank Reactors with High-Activity Soluble Ziegler-Type Catalysts," *J. Appl. Polym. Sci.*, **30**, 2707 (1985).

Choi, K. Y., and W. H. Ray, "The Dynamic Behavior of Continuous Stirred Bed Reactors for the Solid Catalyzed Gas Phase Polymerization of Propylene," *Chem. Eng. Sci.*, **43**(10), 2587 (1988).

Choi, K. Y., and W. H. Ray, "The Dynamic Behavior of a Fluidized-Bed Reactor for Solid Catalyzed Gas-Phase Olefin Polymerization," *Chem. Eng. Sci.*, **40**(12), 2261 (1985).

Cozewith, C., "Transient Response of Continuous-Flow Stirred Tank Polymerization Reactors," *AIChE J.*, **34**(2), 272 (1988).

Machon, J. P., "Ethylene Polymerization at High Temperature with Ziegler-Natta Catalysts," *Transition Metal Catalyzed Polymerizations*, p. 344, R. P. Quirk, ed., Cambridge Univ. Press, Cambridge, U.K. (1988).

Ray, W. H., "On the Mathematical Modeling of Polymerization Reactors," *J. Macromol. Sci.—Revs. Macromol. Chem.*, **C8**(1), 1 (1972).



*Manuscript received Mar. 7, 1991, and revision received July 9, 1991.*